Original Article

Metabolomics studies of prostate cancer using gas chromatography-mass spectrometery

Hua Xin[1], Wei-Qun Wang[2], Zhi-Wei Yang[2], Jun-Xing Liu[2], Sheng Li[1], Lin Wang[1], Qing-Lin Jiang[2], Lin-Lin Jia[2]

[1]Department of Laboratory Medicine, The First Affiliated Hospital of Jiamusi University, Jiamusi 154003, China; [2]School of Basic Medical Science, Jiamusi University, Jiamusi 154007, China

Contributions: (I) Conception and design: H Xin, L Wang, QL Jiang; (II) Administrative support: L Wang, QL Jiang; (III) Provision of study materials or patients: WQ Wang, ZW Yang, JX Liu; (IV) Collection and assembly of data: S Li, LL Jia; (V) Data analysis and interpretation: WQ Wang, JX Liu, LL Jia; (VI) Manuscript writing: All authors; (VII) Final approval of manuscript: All authors.

Correspondence to: Lin Wang. Department of Laboratory Medicine, The First Affiliated Hospital of Jiamusi University, Jiamusi 154003, China. Email: wanglin4477@163.com; Qing-Lin Jiang. School of Basic Medical Science, Jiamusi University, Jiamusi 154007, China. Email: jqljms@126.com.

Background: Metabolomics is a powerful analytical approach that is widely used for early diagnosis of many tumors. In this study, we performed a comparative metabolomics analysis to identify metabolic differences in prostate cancer.

Methods: We applied gas chromatography-mass spectrometry (GC-MS) to analyze the metabolic differences between normal prostate epithelial cells and prostate cancer cells (PC-3, LNCaP, and DU145 cells). We performed pairwise comparisons of the metabolomes for the intracellular and extracellular fluid using principal component analysis (PCA), partial least squares discriminant analysis (PLS-DA), and Student's *t*-test.

Results: Our results revealed significantly different expression patterns among the metabolite groups, including amino acids, organic acids, sugars, and cholesterol. Of these four categories, cholesterol showed potential for combination with prostate-specific antigen (PSA) to improve diagnosis of prostate cancer.

Conclusions: GC-MS may be an effective approach to reduce the frequency of invasive biopsies. Analysis of the diagnostic significance of prostate cancer markers will help to identify more meaningful tumor markers for prostate cancer diagnosis and treatment, contribute to the understanding of the pathogenesis of prostate cancer, and provide the basis for new ideas.

Keywords: Prostate cancer; metabolomics; cholesterol metabolism; gas chromatography-mass spectrometery (GC-MS); tumor biomarker

Submitted May 03, 2016. Accepted for publication May 31, 2016.
doi: 10.21037/tcr.2016.06.15
View this article at: http://dx.doi.org/10.21037/tcr.2016.06.15

Introduction

There have been numerous clinical studies into the methods for early tumor diagnosis, including identifying tumor markers and pathology, ultrasonic techniques, and nuclear magnetic resonance. Despite these advances, many patients are still diagnosed with advanced or metastatic cancer after the optimum treatment point (1,2). Therefore, identification of additional biomarkers or development of new technologies that allow early diagnosis of cancers remains an important issue.

Recently, metabolomics has attracted increasing attention and been widely used for early cancer diagnosis (3). The occurrence and development of tumors in the human body inevitably cause changes in metabolites, and nucleotide metabolism has been suggested as a cancer marker (4). In clinical practice, more than three-quarters of patients with ovarian cancer were diagnosed with advanced cancer and must undergo surgical removal and chemotherapy. Even

with intensive therapy, about one-half of these patients experienced relapse within 2 years (5). However, early diagnosis of ovarian cancer would greatly improve the patient survival rate (6). A previous study showed that combination of the tumor markers CA125, CA72-4, CA15-3, and M-CSF and detection through artificial neural network analysis improved the accuracy of early diagnosis of ovarian cancer; the specificity of this method reached 98% with 71% sensitivity compared to 46% sensitivity for CA125 alone (7). In addition, metabolomics testing has been applied in the early diagnosis of breast cancer, illustrating that metabolomics analysis can provide broader more screening indicators (8).

Prostate cancer mainly occurs in middle-aged men and is often diagnosed at late stage. Thus, early diagnosis of prostate cancer would have far-reaching significance for patients (9,10). With the aid of high-throughput liquid/gas chromatography-mass spectrometry (LC/GC-MS), a metabolomics study performed on 262 clinical prostate cancer specimens identified 1,126 intermediate metabolites (10). For example, creatinine levels gradually increased from early to metastatic prostate cancer, and sarcosine was detected in rectal specimens from patients with prostate cancer, suggesting that LC/GC-MS is an effective method for early diagnosis and clinical staging of prostate cancer.

Current cancer therapeutics is mainly directed against tumor cells, targeting development and growth processes, proliferation, and metastasis arising from abnormal pathways. Metabolomics can help to identify key metabolites during the development of the tumor and improve the efficacy by tumor targeted therapy, thereby establishing a new direction for research and clinical applications (11). The most important evaluation of this application is identification of metabolic biomarkers for cancer diagnosis and prognosis. Recently, the application of magnetic resonance spectroscopy imaging (MRSI) technologies for tumor evaluation has attracted a lot of attention (12). However, in clinical work, the co-existence of breast cancer with metabolic or other integrated disease such as insulin resistance, obesity, hypertension, or dyslipidemia will result in relatively poor diagnosis (13).

In this study, metabolic differences between normal prostate epithelial cells and prostate cancer cells at various stages were analyzed with GC-MS to identify prostate cancer-specific metabolites. The analysis of prostate cancer markers with diagnostic significance will provide more meaningful tumor biomarkers for prostate cancer diagnosis and treatment, further our understanding of prostate cancer pathogenesis, and establish a foundation for new ideas.

Methods

Materials

Reagents for cell growth media (e.g., Leibovitz's L-15 medium, RPMI medium 1640, epidermal growth factor, Ham's F-12 nutrient mixture, McCoy's 5A medium) and methanol were purchased from CNW Technologies GmbH (Germany). Other commercially available reagents were analytical grade. Derivatives reagents were purchased from AMP (USA). Watsons distilled water was used for all experimental equipment.

Growth medium

Dulbecco's Modified Eagle's Medium (DMEM) containing 80–90% basal medium supplemented with 10–20% fetal bovine serum and 1% bis anti-stock solution (penicillin and streptomycin) were purchased from Gibco (USA). The final concentrations of penicillin and streptomycin were 100 U/mL and 100 μg/mL, respectively (10).

Cell culture

Prostate cancer cell lines PC-3, DU145, and LNCaP and the normal prostate epithelial cell line RWPE were purchased from the American Type Culture Collection (ATCC, USA). The cell lines were cultured in DMEM at 37 ℃ in 5% CO_2 under sterile conditions as previously described (14,15). The filtered culture supernatant was stored in a sealed bottle at 4 ℃ (16).

Sample grouping

The samples of normal human prostate epithelial cells (RWPE cells), normal human prostate epithelial extracellular fluid (RWPE solution), androgen-independent human prostate cancer cells (DU145 cells), androgen-independent human prostate cancer cells extracellular fluid (DU145 solution), androgen-dependent LNCaP human prostate cancer cells (LNCaP cells), androgen-dependent LNCaP human prostate cancer cells extracellular fluid (LNCaP solution), androgen-independent PC-3 human prostate cancer cells (PC-3 cells), and androgen-independent PC-3 human prostate cancer cells extracellular

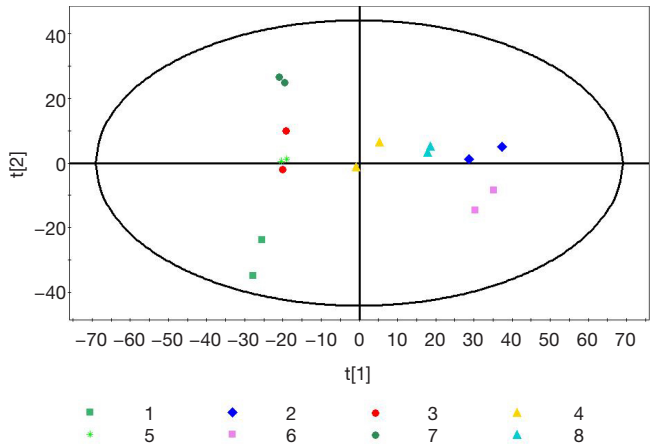

Figure 1 PCA plot for each group. The sample numbers used in the PCA plot for group 1, 2, 3, 4, 5, 6, 7 and 8 are two, respectively. The PCA plot is generated by analyzing the principle component with Simca-P13.0 after drawing the peak information matrix extracted from the total ion graph. PCA, principal component analysis.

fluid (PC-3 solution) were divided into groups 1, 2, 3, 4, 5, 6, 7 and 8, respectively (n=2 each). Group 9 was included as a quality control and indicates instrument stability during the detection process.

GC-MS analysis

A 200-μL sample was used for GC-MS metabolomic analysis on an Agilent 7890A/5975C GC-MS as previously described (17) using an Agilent J&W HP-5ms capillary column (30 m × 0.25 mm × 0.25 μm). Instrument parameters were set as follows: inlet temperature, 280 ℃; electrospray ionization ion source temperature, 230 ℃; quadrupole temperature, 150 ℃; carrier gas, high-purity helium (purity greater than 99.999%); splitless injection volume, 1.0 μL (18). The following temperature program was used: 80 ℃ for 2 min, increase to 320 ℃ at 10 ℃/min, and maintain at 320 ℃ for 6 min. Mass spectra were collected in full scan mode from m/z 50–550. Random sequences of consecutive samples were analyzed to avoid random errors from instrumental signal fluctuations (19). Calculation of the fold change: First, we calculated the difference in the mean value of the peak intensity for metabolites in two groups and the ratio between the mean value of the two groups. Then we calculated the log2 value of the ratio. The final result indicates the fold change. Positive values indicate significant metabolites differences between the two groups, and negative values indicate the opposite.

Data analysis

The data were analyzed in R using the XCMS software package for GC-MS data preprocessing (20), including removal of column bleed and impurity peaks introduced during sample preparation. The final result was stored as a two-dimensional data matrix including each observable (sample) and peak intensities (21). All data were normalized to the total signal integration. The data matrix was edited using Simca-P software (version 13.0) and analyzed using principal component analysis (PCA). The data of the metabolomes in extracellular and intracellular fluid were analyzed by PCA, partial least squares discriminant analysis (PLS-DA), and Student's *t*-test. A P value <0.05 was considered significant.

Results

Overall analysis

We recovered 1,474 samples of fragment ion. Metabolic differences within a group and comparisons between samples were determined by body composition analysis. The most intuitive data format is unit variance (UV) scaling and mean-centering after formal analysis in Simca-P. However, differences between groups were analyzed using PCA. We identified two main components with cumulative R^2X =0.568 and Q^2 =0.409. The PCA score plot is shown in *Figure 1*. R^2X is a non-supervisory metric that indicates the quality of the PCA model for identifying the main parameters. When R^2X is greater than 0.4, the modeling is reliable. Differences in metabolism can be explained using PCA in combination with relative PLS-DA to reflect real differences in the experimental group in the middle of the figure (*Figure 1*).

Metabolic differences between groups 1 and 2

The differences of metabolites were compared between group 1 (RWPE cells) and group 2 (RWPE solution). PCA identified two main components accounting for metabolic differences between the groups with cumulative R^2X =0.918 and Q^2 =0.612. To uncover any significant differences in metabolite levels, we used supervisory PLS-DA. The PLS-DA score plot showed significant differences between the two groups, and we calculated the variable influence on projection (VIP) scores using an orthogonal (O) PLS-

Table 1 Metabolic differences between groups 1 and 2

VIP	m/z	rt (min)	Name	P value	Fold change (2/1)
1.095	373	11.73	5-pentanediamine	0.023	–1.777
1.098	342	13.94	D-erythro-pentitol	0.021	3.090
1.102	75	7.70	1,2-bis(hydroxymethyl) cyclohexane	0.017	1.025
1.121	174	12.84	1H-indole-3-ethylamine	0.000	2.460
1.115	200	8.78	3-methylvalerate	0.005	8.341
1.074	407	16.68	4-amino-1-oxo-1,2-dihydrophthalazine	0.042	8.144
1.075	341	12.72	4-aminobutyric acid	0.041	2.452
1.112	311	7.28	4-hydroxybenzoxazolone	0.008	1.590
1.121	174	12.67	A-aminoisobutyrate	0.000	2.449
1.087	392	8.23	A-hydroxybutyric acid	0.030	–0.675
1.083	166	6.80	A-hydroxycyclohexene	0.034	–0.400
1.099	341	20.12	Eicosanoids	0.019	–4.755
1.071	103	17.12	D-fructose	0.044	8.418
1.121	129	17.27	D-galactose	0.000	5.082
1.121	133	17.52	D-glucitol	0.000	7.972
1.118	157	16.76	D-glucose	0.002	8.959
1.121	117	17.44	D-mannose	0.000	7.861
1.106	339	19.94	Estradiol	0.013	–3.925
1.097	221	5.92	Glycol	0.022	–2.814
1.121	103	17.71	Galactose	0.000	5.391
1.074	325	10.57	Glycerate	0.042	0.771
1.108	205	9.81	Glycerin	0.012	1.154
1.078	174	10.27	Glycine	0.039	4.965
1.090	174	12.23	Glycylglycine	0.027	2.595
1.068	188	8.66	Glyoxylate	0.047	2.453
1.110	144	11.61	Homocysteine	0.010	2.218
1.108	432	19.14	Inositol	0.012	1.144
1.120	86	8.44	Isoleucine	0.000	5.301
1.121	147	6.88	Lactate	0.000	2.702
1.070	226	16.49	L-asparagine	0.045	–6.774
1.120	86	8.13	Leucine	0.001	5.246
1.120	72	7.22	L-valine	0.001	4.333
1.082	242	19.67	N-acetylglucosamine	0.034	–1.303
1.079	232	7.97	Oxalic acid	0.037	3.896
1.121	60	17.62	Palmitic acid	0.000	2.610
1.086	180	9.86	Phosphate	0.031	0.457
1.121	447	13.34	Pregn-5-en-11-one	0.000	–1.093
1.120	319	15.44	Ribitol	0.001	–3.022
1.081	132	9.56	Serine	0.036	4.254
1.106	96	12.48	Fine	0.013	2.682
1.117	284	19.46	Stearate	0.003	4.474
1.083	132	18.38	Myristate	0.034	–2.960

VIP, variable importance in the projection; rt, retention time.

DA model and P values using Student's *t*-test. VIP >1 and P<0.05 were taken as the thresholds for significance. We identified more than 42 differentially expressed metabolites, mainly sugars, organic acids, and amino acids (*Table 1*), between the groups, indicating differences between the intracellular fluid and extracellular fluid metabolomes of normal prostate epithelial cells.

Metabolic differences between groups 1 and 3

Group 1 was compared with group 3 (DU145 cells) to reveal any differences between the intracellular fluid metabolites. PCA revealed two main components with cumulative R^2X =0.862 and Q^2 =0.341. To reveal any significant differences between the metabolomes of the two groups, further analysis was performed using supervisory PLS-DA. The PLS-DA score plot showed significant differences between the two groups (P<0.05), indicating three main components and a quadrature component specific to the metabolites, and yielded more than 23 differentially expressed metabolites (*Table 2*), including cholesterol, stearic acid, 4-aminobutyric acid, and estradiol.

Metabolic differences between groups 1 and 5

The differences of intracellular fluid metabolites between group 1 and group 5 (LNCaP cells) were compared. PCA determined two main components with cumulative R^2X =0.859 and Q^2 =0.355, revealing metabolic differences

Table 2 Metabolic differences between groups 1 and 3

VIP	m/z	rt (min)	Name	P value	Fold change (3/1)
1.365	69	12.86	1H-indole ethylamine	0.003	1.532
1.341	519	12.73	4-aminobutyric acid	0.020	7.055
1.360	288	12.67	A-aminoisobutyrate	0.006	1.230
1.364	234	6.77	A-hydroxycyclohexene	0.003	2.220
1.361	353	28.29	Cholesterol	0.006	20.429
1.360	180	17.12	Fructose	0.007	3.301
1.361	160	17.27	Galactose	0.006	0.328
1.358	133	17.52	D-sorbitol	0.008	0.315
1.334	376	17.44	D-mannose	0.025	0.026
1.356	262	6.49	D-threo-2,5-hexodiulose	0.009	1.870
1.305	339	19.94	Estradiol	0.047	5.526
1.334	221	5.92	Ethylene glycol	0.025	0.205
1.325	205	17.71	Dulcitol	0.032	0.515
1.319	191	18.01	Glucose	0.036	0.574
1.339	325	10.57	Glycerate	0.021	1.358
1.347	190	9.81	Glycerin	0.016	2.561
1.317	135	19.14	Inositol	0.038	1.779
1.316	76	6.86	Lactate	0.038	1.581
1.365	258	16.46	Asparagine	0.003	0.029
1.351	242	19.67	N-acetylglucosamine	0.013	0.081
1.357	60	17.62	Palmitic acid	0.008	24.400
1.367	147	15.44	Ribitol	0.001	0.102
1.368	60	19.46	Stearate	0.000	28.068

VIP, variable importance in the projection; rt, retention time.

between the groups. PLS-DA further revealed more than 46 metabolites that were significantly different between the two groups (*Table 3*), including cholesterol, glycine, homocysteine, proline, and serine.

Metabolic differences between groups 1 and 7

The differences of intracellular fluid metabolites between group 1 and group 7 (PC-3 cells) were compared. PCA determined two main components with cumulative R^2X =0.88 and Q^2 =0.425. The PLS-DA score plot revealed

Table 3 Metabolic differences between groups 1 and 5

VIP	m/z	rt (min)	Name	P value	Fold change (5/1)
1.260	373	11.73	5-pentanediamine	0.020	–1.362
1.274	69	12.86	1H-indole-3-ethanamine	0.010	0.951
1.253	87	7.18	2-heptanone	0.026	1.730
1.283	173	16.68	4-amino-1-oxo-1,2-dihydrophthalazine	0.002	4.475
1.273	519	12.73	4-aminobutyric acid	0.010	2.593
1.254	151	7.29	4-hydroxybenzoxazolone	0.024	0.287
1.225	169	12.67	A-aminoisobutyrate	0.047	0.476
1.274	96	7.07	Acetic acid	0.009	1.191
1.245	234	6.77	A-hydroxycyclohexene	0.031	1.372
1.236	74	6.72	Alanine	0.038	0.531
1.242	341	20.12	Eicosanoids	0.034	1.342
1.280	353	28.29	Cholesterol	0.004	4.792
1.282	180	17.12	D-fructose	0.003	1.560
1.236	160	17.27	D-galactose	0.039	–0.457
1.274	73	17.52	Sorbitol	0.009	1.508
1.277	160	16.76	D-glucose	0.007	1.032
1.273	262	6.49	D-threo-2,5-hexodiulose	0.010	0.874
1.266	339	19.94	Estradiol	0.015	1.497
1.246	221	5.92	Glycol	0.031	–1.812
1.235	103	17.71	Dulcitol	0.040	–0.866
1.283	346	18.11	Glucose	0.002	–1.719
1.276	325	10.57	Glycerate	0.007	0.629
1.266	72	9.82	Glycerin	0.015	0.944
1.282	174	10.27	Glycine	0.003	4.073
1.265	162	12.23	Glycylglycine	0.016	2.830
1.266	216	8.66	Glyoxylate	0.015	3.141
1.285	144	11.61	Homocysteine	0.001	8.610
1.283	75	8.44	Isoleucine	0.002	0.777
1.277	76	6.86	Lactate	0.007	0.566
1.285	226	16.49	L-asparagine	0.000	4.281
1.233	86	8.13	Leucine	0.041	1.898
1.281	158	10.08	L-threonine	0.004	4.530
1.250	72	7.22	L-valine	0.028	1.663

Table 3 *(continued)*

Table 3 *(continued)*

VIP	m/z	rt (min)	Name	P value	Fold change (5/1)
1.265	242	19.67	N-acetylglucosamine	0.016	–2.397
1.225	152	7.92	Oxalic acid	0.047	0.526
1.233	60	17.62	Palmitic acid	0.041	2.475
1.235	270	9.86	Phosphate	0.039	–0.223
1.275	450	13.33	Pregn-5-en-11-one	0.009	–1.125
1.265	143	10.15	Proline	0.016	4.371
1.227	174	11.89	Putrescine	0.046	2.336
1.273	240	10.38	Pyrrole-2-carboxylic acid	0.010	3.227
1.283	147	15.44	Ribitol	0.002	–1.334
1.284	132	9.56	Serine	0.001	5.429
1.273	168	12.48	Spermine	0.010	3.225
1.280	60	19.46	Stearate	0.005	2.850
1.228	132	18.38	Myristic	0.045	1.408

VIP, variable importance in the projection; rt, retention time.

significant differences (P<0.05) with two main components and identified more than 36 significant metabolite differences (*Table 4*), with the largest differences for glucose, homocysteine, and serine.

Metabolic differences between groups 2 and 4

The differences of extracellular fluid metabolites fluid metabolites between group 2 and group 4 (DU145 solution) were compared. PCA determined two main principal components with cumulative R^2X =0.83 and Q^2 =0.183. The PLS-DA score plot showed significant differences between the groups and received a master component and a quadrature component (*Table 5*). The appearance of the master component indicates that the main component in the metabolic compound has been extracted, and the quadrature component represents the removal of interferents. The OPLS-DA model identified more than 20 differential metabolites, with significantly elevated cholesterol in group 4 (P<0.05).

Metabolic differences between groups 2 and 6

The differences of extracellular metabolites between group

Table 4 Metabolic differences between groups 1 and 7

VIP	m/z	rt (min)	Name	P value	Fold change (7/1)
1.154	342	13.94	D-red E sugar alcohol	0.047	2.574
1.192	69	12.86	1H-indole ethylamine	0.016	0.900
1.175	87	7.18	2-heptanone	0.030	1.713
1.153	173	16.68	4-amino-1-oxo-2-dihydrophthalazine	0.047	2.280
1.206	519	12.73	4-aminobutyric acid	0.004	2.539
1.200	122	7.29	4-hydroxybenzoxazolone	0.009	0.156
1.153	169	12.67	A-amino isobutyric acid	0.047	0.597
1.200	96	7.07	Acetic acid	0.009	1.173
1.180	234	6.77	A-hydroxycyclohexene	0.025	1.404
1.179	74	6.72	Alanine	0.026	0.625
1.202	180	17.12	D-fructose	0.007	1.869
1.208	160	17.27	D-galactose	0.002	3.116
1.208	73	17.52	Sorbitol	0.002	2.393
1.208	160	16.76	D-glucose	0.002	3.886
1.197	376	17.44	D-mannose	0.011	1.308
1.204	339	19.94	Estradiol	0.006	1.706
1.172	221	5.92	Glycol	0.032	–2.013
1.191	205	17.71	Dulcitol	0.016	–0.801
1.209	346	18.01	Glucose	0.002	4.292
1.210	341	10.57	Glycerate	0.000	0.490
1.197	73	9.82	Glycerin	0.011	0.739
1.156	174	10.27	Glycine	0.045	2.327
1.160	162	12.23	Glycylglycine	0.042	2.787
1.210	144	11.61	Homocysteine	0.000	8.841
1.197	135	19.14	Inositol	0.011	1.103
1.201	75	6.86	Lactate	0.008	0.724
1.205	226	16.49	L-asparagine	0.004	2.148
1.158	72	7.22	L-valine	0.044	1.331
1.188	243	19.67	N-acetylglucosamine	0.018	–2.782
1.157	286	9.86	Phosphate	0.044	–0.432
1.208	450	13.33	Pregn-5-en-11-one	0.002	–1.429
1.209	147	15.44	Ribitol	0.001	–2.310
1.181	132	9.56	Serine	0.024	3.069
1.173	168	12.48	Spermine	0.031	3.192
1.209	60	19.46	Stearate	0.001	2.743
1.160	325	10.33	Succinic acid	0.042	0.425

VIP, variable importance in the projection; rt, retention time.

Table 5 Metabolic differences between groups 2 and 4

VIP	m/z	rt (min)	Name	P value	Fold change (4/2)
1.436	75	7.70	1,2-bis(hydroxymethyl) cyclohexane	0.004	−0.811
1.406	311	7.28	4-hydroxybenzoxazolone	0.016	−1.318
1.256	316	28.19	Cholesterol	0.006	3.878
1.441	173	17.12	D-fructose	0.014	−1.831
1.257	161	17.38	D-galactose	0.000	−10.707
1.442	73	17.52	D-glucitol	0.001	−2.004
1.118	160	16.76	D-glucose	0.002	−8.283
1.219	376	17.44	D-mannose	0.000	−9.476
1.372	262	5.92	Glycol	0.021	0.776
1.424	183	17.71	Galactose	0.019	−0.228
1.402	220	9.81	Glycerin	0.046	0.354
1.230	290	14.75	Indolepropionate	0.004	−2.827
1.014	178	19.14	Inositol	0.041	−0.172
1.203	56	8.45	Isoleucine	0.010	−0.839
1.440	76	6.86	Lactate	0.038	−0.206
1.426	61	8.14	Leucine	0.003	−0.446
1.428	72	7.22	L-valine	0.011	−0.915
1.307	242	19.67	N-acetylglucosamine	0.018	−3.630
1.324	400	24.38	Oleic acid amide	0.030	−2.499
1.442	147	15.44	Ribitol	0.047	−0.691

VIP, variable importance in the projection; rt, retention time.

Table 6 Metabolic differences between groups 2 and 6

VIP	m/z	rt (min)	Name	P value	Fold change (6/2)
1.436	75	7.70	1,2-bis(hydroxymethyl) cyclohexane	0.004	−0.437
1.431	293	12.86	1H-indole-3-ethylamine	0.008	−0.216
1.429	200	8.78	3-methacrylic acid	0.009	−2.202
1.406	311	7.28	4-hydroxybenzoxazolone	0.025	−0.858
1.440	74	6.72	Alanine	0.002	1.722
1.388	342	20.13	Eicosanoids	0.038	0.950
1.431	443	28.29	Cholesterol	0.008	4.036
1.441	173	17.12	D-fructose	0.001	1.255
1.438	168	17.38	D-galactose	0.003	0.310
1.442	73	17.52	D-glucitol	0.000	1.768
1.380	392	16.78	D-glucose	0.043	0.540
1.404	343	17.44	D-mannose	0.027	0.212
1.372	262	5.92	Glycol	0.049	0.538
1.424	183	17.71	Galactose	0.013	−0.271
1.402	220	9.81	Glycerin	0.028	−0.483
1.385	144	11.61	Homocysteine	0.040	0.294
1.440	76	6.86	Lactate	0.001	−1.001
1.436	182	16.49	L-asparagine	0.005	−0.281
1.426	61	8.14	Leucine	0.012	0.468
1.428	72	7.22	L-valine	0.010	0.645
1.389	167	7.92	Oxalic acid	0.037	−0.107
1.407	60	17.62	Palmitic acid	0.025	−0.150
1.404	451	13.33	Pregn-5-en-11-one	0.027	−0.413
1.442	147	15.44	Ribitol	0.001	2.388
1.426	132	9.56	Serine	0.011	2.005
1.419	132	18.38	Myristate	0.016	1.014

VIP, variable importance in the projection; rt, retention time.

2 and group 6 (LNCaP solution) were compared. PCA determined two main components with cumulative R^2X =0.822 and Q^2 =−0.0154, indicating significant metabolic differences between the two groups (P<0.05). The PLS-DA score plot indicated significant difference between the two groups and received a master component and a quadrature component (*Table 6*). Fifteen metabolites were significantly increased in group 6 relative to group 2, including cholesterol, serine, alanine, and saccharides.

Metabolic differences between groups 2 and 8

The differences of extracellular metabolites between group 2 and group 8 (PC-3 solution) were compared. Two principal components were obtained with cumulative R^2X =0.888 and Q^2 =0.54 by PCA. The PLS-DA score plot demonstrated significant differences (P<0.05) between the two groups and received a master component and a quadrature component. More than 30 significantly different metabolites were identified (*Table 7*) with 10 increased in group 8, including cholesterol, alanine, serine, stearic acid,

Table 7 Metabolic differences between groups 2 and 8

VIP	m/z	rt (min)	Name	P value	Fold change (8/2)
1.296	75	7.702	1,2-bis(hydroxymethyl) cyclohexene	0.002	−0.819
1.255	293	12.865	1H-indole ethylamine	0.034	−0.392
1.245	200	8.776	3-methylpentanoic acid	0.042	−0.857
1.257	311	7.280	4-hydroxybenzoxazolone	0.032	−1.017
1.256	169	12.667	A-aminoisobutyric acid	0.033	−0.144
1.269	234	6.771	Cholesterol	0.024	3.063
1.297	74	6.724	Alanine	0.002	1.727
1.297	342	20.131	Eicosanoids	0.002	2.559
1.297	173	17.125	Fructose	0.002	−1.652
1.285	168	17.381	Galactose	0.011	−0.986
1.290	73	17.518	D-sorbitol	0.007	−0.585
1.296	343	17.440	D-mannose	0.002	−1.002
1.266	262	5.920	Ethylene glycol	0.026	0.709
1.265	322	17.710	Dulcitol	0.026	−0.584
1.265	346	18.013	Glucose	0.026	2.363
1.286	104	9.812	Glycerin	0.011	−0.278
1.287	144	11.606	Homocysteine	0.009	−1.051
1.272	181	19.142	Inositol	0.021	−0.154
1.290	56	8.448	Isoleucine	0.007	−0.515
1.266	76	6.860	Lactate	0.026	−0.539
1.281	70	8.140	Leucine	0.014	−0.508
1.276	242	19.672	N-acetylglucosamine	0.018	−3.725
1.279	488	24.384	Oleic acid amide	0.016	−3.109
1.276	235	7.961	Oxalic acid	0.018	2.374
1.253	60	17.616	Palmitic acid	0.035	2.125
1.298	449	13.330	Pregn-5-en-11-one	0.001	−0.940
1.288	147	15.437	Ribitol	0.009	0.722
1.235	159	9.555	Serine	0.050	0.829
1.252	241	19.460	Stearate	0.036	3.386
1.294	132	18.379	Myristate	0.004	1.955

VIP, variable importance in the projection; rt, retention time.

arachidic acid, and carbohydrates.

Metabolic differences between groups 3 and 4

The differences of metabolites were compared between group 3 and group 4. PCA determined two main components with cumulative R^2X =0.823 and Q^2 =0.102, indicating significant metabolic differences between the two groups ($P<0.05$). Furthermore, the PLS-DA score plot revealed significant differences and received a master component and a quadrature component. The OPLS-DA model identified 27 significantly different metabolites (*Table 8*), with galactose, sugars, leucine, L-valine, and phosphoric acid significantly increased.

Metabolic differences between groups 5 and 6

The differences of metabolites were compared between group 5 and group 6. PCA determined two main components with cumulative R^2X =0.898 and Q^2 =0.521, indicating significant metabolic differences between the two groups ($P<0.05$). A PLS-DA score plot showed significant differences and received a master component and a quadrature component. More than 37 differentially expressed metabolites were identified (*Table 9*), with 20 increased in the extracellular fluid, including sugars, L-valine, leucine, and 3-methylvaleric acid.

Metabolic differences between groups 7 and 8

The differences of metabolites were compared between group 7 and group 8. PCA determined two main components with cumulative R^2X =0.921 and Q^2 =0.661. The PLS-DA score plot indicated significant differences between the two groups and received a master component and a quadrature component. The OPLS-DA model identified more than 40 differences in metabolites (*Table 10*), including carbohydrates, glycine, leucine, serine, L-threonine, and other organic acids.

Discussion

Metabolomics can reveal the metabolic microenvironment

Table 8 Metabolic differences between groups 3 and 4

VIP	m/z	rt (min)	Name	P value	Fold change (4/3)
1.291	66	7.702	1,2-bis(hydroxymethyl) cyclohexane	0.032	0.623
1.307	69	12.859	1H-indole-3-ethylamine	0.020	2.532
1.302	200	8.776	3-methylvalerate	0.024	7.025
1.334	233	8.205	A-hydroxy butyrate	0.000	6.831
1.291	166	6.802	A-hydroxycyclohexene	0.032	–0.566
1.310	74	6.724	Alanine	0.018	–2.010
1.290	341	20.124	Eicosanoids	0.032	–2.005
1.326	353	28.288	Cholesterol	0.006	–7.547
1.271	180	17.120	D-fructose	0.047	3.076
1.333	129	17.270	D-galactose	0.000	4.508
1.325	73	17.518	D-glucitol	0.007	5.277
1.293	157	16.762	D-glucose	0.031	2.473
1.272	262	6.487	D-threo-2,5-hexodiulose	0.046	–1.328
1.286	339	19.945	Estradiol	0.035	–4.403
1.325	103	17.710	Galactose	0.006	5.733
1.295	345	18.011	Glucopyranose	0.029	–3.094
1.308	325	10.573	Glycerate	0.019	0.389
1.295	72	9.820	Glycerin	0.029	–0.236
1.283	135	19.139	Inositol	0.038	–0.501
1.322	75	8.436	Isoleucine	0.009	1.327
1.331	73	6.867	Lactate	0.002	1.513
1.317	226	16.494	L-asparagine	0.012	–7.652
1.310	86	8.134	Leucine	0.018	4.021
1.316	72	7.222	L-valine	0.013	3.063
1.308	138	9.875	Phosphate	0.019	2.555
1.276	323	15.434	Ribitol	0.043	1.369
1.272	284	19.460	Stearate	0.046	–1.326

VIP, variable importance in the projection; rt, retention time.

Table 9 Metabolic differences between groups 5 and 6

VIP	m/z	rt (min)	Name	P value	Fold change (6/5)
1.126	373	11.73	5-norvaline	0.018	0.017
1.145	69	12.86	1H-indole-3-ethylamine	0.001	2.541
1.146	384	22.97	1-monopalmitate	0.000	–0.453
1.140	87	7.18	2-heptanone	0.006	–2.297
1.092	181	7.12	2-pentanone	0.048	–0.112
1.130	200	8.78	3-methylvalerate	0.014	8.457
1.146	174	12.67	A-aminoisobutyric acid	0.001	1.935
1.146	96	7.07	Acetic acid	0.001	–1.494
1.146	233	8.21	A-hydroxy butyrate	0.000	4.745
1.143	74	6.72	Alanine	0.003	–0.549
1.133	341	20.12	Eicosanoids	0.012	–4.202
1.146	180	17.12	D-fructose	0.000	5.810
1.141	129	17.27	D-galactose	0.004	5.324
1.146	133	17.52	D-glucitol	0.000	7.903
1.144	157	16.76	D-glucose	0.002	8.845
1.146	117	17.44	D-mannose	0.000	8.672
1.122	262	6.49	D-threo-2,5-hexodiulose	0.021	–0.745
1.140	339	19.94	Estradiol	0.006	–4.588
1.125	221	5.92	Glycol	0.019	–0.956
1.145	103	17.71	Galactose	0.001	6.093
1.146	72	9.82	Glycerin	0.001	–1.347
1.108	174	10.27	Glycine	0.033	0.574
1.102	162	12.23	Glycylglycine	0.038	–1.107
1.105	216	8.66	Glyoxylate	0.036	–0.335
1.146	144	11.61	Homocysteine	0.001	–6.097
1.133	319	19.14	Inositol	0.012	0.680
1.146	75	8.44	Isoleucine	0.000	1.795
1.144	73	6.87	Lactate	0.002	0.766
1.146	226	16.49	L-asparagine	0.000	–10.587
1.146	86	8.13	Leucine	0.001	3.879
1.145	72	7.22	L-valine	0.001	3.315
1.142	314	9.87	Phosphate	0.004	0.655
1.094	240	10.38	Pyrrole-2-carboxylic acid	0.046	–0.687
1.144	323	15.43	Ribitol	0.002	2.090
1.119	132	9.56	Serine	0.024	0.830
1.123	284	19.46	Stearate	0.021	–2.240
1.126	132	18.38	Myristate	0.018	–3.354

VIP, variable importance in the projection; rt, retention time.

Table 10 Metabolic differences between groups 7 and 8

VIP	m/z	rt (min)	Name	P value	Fold change (6/5)
1.110	75	7.70	1,2-bis(hydroxymethyl) cyclohexane	0.028	−0.247
1.137	69	12.86	1H-indole-3-ethylamine	0.004	2.401
1.125	87	7.18	Heptanone	0.014	−2.163
1.127	200	8.78	3-methylvalerate	0.013	7.615
1.113	173	16.68	4-amino-1-oxo-1,2-dihydrophthalazine	0.025	0.680
1.107	519	12.73	4-aminobutyric acid	0.030	0.385
1.139	174	12.67	A-aminoisobutyric acid	0.002	1.688
1.097	96	7.07	Acetic acid	0.038	−0.527
1.138	233	8.21	A-hydroxy butyrate	0.003	4.557
1.119	234	6.77	A-hydroxycyclohexene	0.019	2.970
1.097	459	16.22	Arabinofuranosyl	0.039	0.488
1.141	180	17.12	D-fructose	0.000	3.416
1.136	129	17.27	D-galactose	0.005	2.826
1.127	133	17.52	D-glucitol	0.013	2.868
1.141	157	16.76	D-glucose	0.000	4.738
1.141	117	17.44	D-mannose	0.000	5.802
1.139	339	19.94	Estradiol	0.002	−4.824
1.119	58	5.94	Glycol	0.020	1.703
1.137	103	17.71	Galactose	0.004	5.279
1.132	204	18.01	Glucopyranose	0.009	7.922
1.135	341	10.57	Glycerate	0.006	0.378
1.128	72	9.82	Glycerin	0.012	−0.412
1.141	174	10.27	Glycine	0.001	2.028
1.111	216	8.66	Glyoxylate	0.026	0.628
1.141	144	11.61	Homocysteine	0.000	−7.673
1.137	135	19.14	Inositol	0.004	−0.791
1.137	75	8.44	Isoleucine	0.004	1.013
1.139	73	6.87	Lactate	0.002	1.162
1.141	226	16.49	L-asparagine	0.000	−8.607
1.133	86	8.13	Leucine	0.007	2.486
1.125	144	9.00	L-norvaline	0.015	4.558
1.129	158	10.08	L-threonine	0.011	4.488
1.141	72	7.22	L-valine	0.000	2.901
1.109	60	17.62	Palmitic acid	0.028	2.959
1.136	314	9.87	Phosphate	0.005	0.750
1.114	450	13.33	Pregn-5-en-11-one	0.024	−0.853
1.107	240	10.38	Pyrrole-2-carboxylic acid	0.030	1.075
1.121	147	15.44	Ribitol	0.018	0.744
1.138	132	9.56	Serine	0.003	2.024
1.121	341	10.33	Succinic acid	0.018	0.452

VIP, variable importance in the projection; rt, retention time.

of cells, thereby identifying changes in gene regulation and metabolic activity and reactions (22,23). Tumor cell metabolism is inseparable from the surroundings because tumor cell growth requires key metabolites from the microenvironment (24-27). In evaluating the diagnosis, prognosis, and therapeutic efficacy for a disease, biomarkers play an increasingly important role. GC-MS-based metabolomics analyses have potential effects in evaluating the development of cancer through metabolic screening and earlier identification of more sensitive diagnostic markers (24-27). In this study, we found significant differences in metabolite expression between prostate cancer cells and normal prostate epithelial cells. These biomarkers, including cholesterol, amino acid, homocysteine, proline, serine, alanine, and saccharides, showed significantly different average levels between tumor groups and the normal control group; detection of the intracellular and extracellular fluids showed good consistency.

Cholesterol was identified with a relatively high significance in all comparisons. Therefore, we focused on the role of cholesterol metabolism in the growth of prostate cancer cells. Cholesterol is an important building block for cell membranes, synthesis of bile acids, vitamin D, raw steroid hormones, and their derivatives (28). Acetyl-CoA is the starting material for forming isopentenyl pyrophosphate (IPP), which is converted into squalene and subsequently into cholesterol. As a synthetic steroid hormone precursor, cholesterol can be enzymatically converted into androgens, which may affect the androgen receptor signaling pathway and promote the acceptance of androgen deprivation therapy for prostate cancer patients with castration-resistant tumor growth (29,30). High physiological cholesterol levels

can promote androgen synthesis in the prostate gland, and studies have demonstrated a connection between the occurrence of prostate cancer and high cholesterol levels (31). Rapid reproduction of tumor cells might also be associated with high cholesterol levels, as previous studies showed that artificially raising cholesterol levels promoted prostate cancer proliferation, migration, and invasion, whereas lowering cholesterol levels and interfering with growth factor signaling pathways could induce tumor cell apoptosis (29,30).

Glucose was also significantly increased in prostate cancer groups herein. A previous report indicated that patients with diabetes for 2–5 years exhibited increased incidence of prostate cancer; thus, patients with diabetes should pay attention to cholesterol levels in screening for prostate cancer (32). Because tumor cell energy metabolism occurs mainly through anaerobic glycolysis of glucose, hyperglycemia will promote tumor cell growth. Furthermore, long-term exposure to elevated blood sugar levels can gradually thicken the basement membrane of capillaries, decrease the permeability, impair mitochondrial respiratory enzymes and cellular respiration barriers, and increase glycolysis, which ultimately selects for tumor cells (33).

The serine protease hepsin and cysteine-rich secretory protein 3 (CRISP3) have been reported as diagnostic markers for prostate cancer. Immunohistochemical studies demonstrated high concentrations of serine protease in prostate cancer and prostatic intraepithelial neoplasia (PIN) (34). CRISP3 is a secreted protein produced in the male reproductive tract and is present at high levels in seminal plasma samples. Immunohistochemical staining of prostate tissue showed high levels of CRISP3 in PIN and prostate cancer samples. The relationship between CRISP3 and prostate cancer accompanied by radical prostatectomy in patients with tissue micro-β1 protamine was evaluated, and CRISP3 was identified as an independent predictor for prostate cancer recurrence (35,36).

In summary, our results showed that GC-MS-based metabolomics comparison of normal prostate epithelial cells and prostate cancer cells could reveal similarities and differences in prostate cancer-specific capture. Our OPLS-DA pairwise modeling analysis, combined with Student's *t*-test, identified significant differences in metabolite expression, including amino acids, organic acids, sugars, and cholesterol. Of the four categories, combined with prostate-specific antigen (PSA), cholesterol showed obvious potential as a biomarker for clinical diagnosis of prostate cancer. Furthermore, our pairwise comparisons of the extracellular fluid and intracellular fluid of normal and cancer cells reflected the differences between normal prostate epithelial cells and prostate cancer cells, which could reduce the necessity for invasive biopsy. Thus, metabolomics studies of prostate cancer using GC-MS can help identify more meaningful tumor markers for prostate cancer diagnosis and treatment, facilitate exploration of the pathogenesis of prostate cancer, and provide the basis for new ideas.

Acknowledgments

Funding: This work was supported by grants from the Heilongjiang Province Natural Science Fund Project (No. D201225) and Research Subject of Jiamusi University (No. 12Z1201504, Sz2010-004).

Footnote

Conflicts of Interest: All authors have completed the ICMJE uniform disclosure form (available at http://dx.doi.org/10.21037/tcr.2016.06.15). The authors have no conflicts of interest to declare.

Ethical Statement: The authors are accountable for all aspects of the work in ensuring that questions related to the accuracy or integrity of any part of the work are appropriately investigated and resolved. The study was conducted in accordance with the Declaration of Helsinki (as revised in 2013).

References

1. Mäbert K, Cojoc M, Peitzsch C, et al. Cancer biomarker discovery: current status and future perspectives. Int J Radiat Biol 2014;90:659-77.
2. Rubin G, Berendsen A, Crawford SM, et al. The expanding role of primary care in cancer control. Lancet Oncol 2015;16:1231-72.

3. Athersuch T. Metabolome analyses in exposome studies: Profiling methods for a vast chemical space. Arch Biochem Biophys 2016;589:177-86.
4. Cheng YS, Xu F. Anticancer function of polyinosinic-polycytidylic acid. Cancer Biol Ther 2010;10:1219-23.
5. Donahue RN, McLaughlin PJ, Zagon IS. Low-dose naltrexone suppresses ovarian cancer and exhibits enhanced inhibition in combination with cisplatin. Exp Biol Med (Maywood) 2011;236:883-95.
6. Menon U, Jacobs IJ. Recent developments in ovarian cancer screening. Curr Opin Obstet Gynecol 2000;12:39-42.
7. Zhang Z, Yu Y, Xu F, et al. Combining multiple serum tumor markers improves detection of stage I epithelial ovarian cancer. Gynecol Oncol 2007;107:526-31.
8. Chan DA, Sutphin PD, Nguyen P, et al. Targeting GLUT1 and the Warburg effect in renal cell carcinoma by chemical synthetic lethality. Sci Transl Med 2011;3:94ra70.
9. Beheshti M, Vali R, Waldenberger P, et al. Detection of bone metastases in patients with prostate cancer by 18F fluorocholine and 18F fluoride PET-CT: a comparative study. Eur J Nucl Med Mol Imaging 2008;35:1766-74.
10. Sreekumar A, Poisson LM, Rajendiran TM, et al. Metabolomic profiles delineate potential role for sarcosine in prostate cancer progression. Nature 2009;457:910-4.
11. Evelhoch J, Garwood M, Vigneron D, et al. Expanding the use of magnetic resonance in the assessment of tumor response to therapy: workshop report. Cancer Res 2005;65:7041-4.
12. Rosen MA, Schnall MD. Dynamic contrast-enhanced magnetic resonance imaging for assessing tumor vascularity and vascular effects of targeted therapies in renal cell carcinoma. Clin Cancer Res 2007;13:770s-776s.
13. Healy LA, Ryan AM, Carroll P, et al. Metabolic syndrome, central obesity and insulin resistance are associated with adverse pathological features in postmenopausal breast cancer. Clin Oncol (R Coll Radiol) 2010;22:281-8.
14. Giangreco AA, Dambal S, Wagner D, et al. Differential expression and regulation of vitamin D hydroxylases and inflammatory genes in prostate stroma and epithelium by 1,25-dihydroxyvitamin D in men with prostate cancer and an in vitro model. J Steroid Biochem Mol Biol 2015;148:156-65.
15. Mikyšková R, Štěpánek I, Indrová M, et al. Dendritic cells pulsed with tumor cells killed by high hydrostatic pressure induce strong immune responses and display therapeutic effects both in murine TC-1 and TRAMP-C2 tumors when combined with docetaxel chemotherapy. Int J Oncol 2016;48:953-64.
16. Phuyal S, Skotland T, Hessvik NP, et al. The ether lipid precursor hexadecylglycerol stimulates the release and changes the composition of exosomes derived from PC-3 cells. J Biol Chem 2015;290:4225-37.
17. Wilton JH, Titus MA, Efstathiou E, et al. Androgenic biomarker prof|ling in human matrices and cell culture samples using high throughput, electrospray tandem mass spectrometry. Prostate 2014;74:722-31.
18. Ueda K, Tatsuguchi A, Saichi N, et al. Plasma low-molecular-weight proteome profiling identified neuropeptide-Y as a prostate cancer biomarker polypeptide. J Proteome Res 2013;12:4497-506.
19. Brennan JC, Denison MS, Holstege DM, et al. 2,3-cis-2R,3R-(-)-epiafzelechin-3-O-p-coumarate, a novel flavan-3-ol isolated from Fallopia convolvulus seed, is an estrogen receptor agonist in human cell lines. BMC Complement Altern Med 2013;13:133.
20. Uppal K, Soltow QA, Strobel FH, et al. xMSanalyzer: automated pipeline for improved feature detection and downstream analysis of large-scale, non-targeted metabolomics data. BMC Bioinformatics 2013;14:15.
21. Huang X, Chen YJ, Cho K, et al. X13CMS: global tracking of isotopic labels in untargeted metabolomics. Anal Chem 2014;86:1632-9.
22. Mendes P, Kell DB, Westerhoff HV. Channelling can decrease pool size. Eur J Biochem 1992;204:257-66.
23. Mendes P, Kell DB, Westerhoff HV. Why and when channelling can decrease pool size at constant net flux in a simple dynamic channel. Biochim Biophys Acta 1996;1289:175-86.
24. Azmi AS, Bao B, Sarkar FH. Exosomes in cancer development, metastasis, and drug resistance: a comprehensive review. Cancer Metastasis Rev 2013;32:623-42.
25. Hannafon BN, Ding WQ. Intercellular communication by exosome-derived microRNAs in cancer. Int J Mol Sci 2013;14:14240-69.
26. Roma-Rodrigues C, Fernandes AR, Baptista PV. Exosome in tumour microenvironment: overview of the crosstalk between normal and cancer cells. Biomed Res Int 2014;2014:179486.
27. Yu DD, Wu Y, Shen HY, et al. Exosomes in development, metastasis and drug resistance of breast cancer. Cancer Sci 2015;106:959-64.
28. Charlton-Menys V, Durrington PN. Human cholesterol metabolism and therapeutic molecules. Exp Physiol 2008;93:27-42.
29. Dillard PR, Lin MF, Khan SA. Androgen-independent

prostate cancer cells acquire the complete steroidogenic potential of synthesizing testosterone from cholesterol. Mol Cell Endocrinol 2008;295:115-20.
30. Montgomery RB, Mostaghel EA, Vessella R, et al. Maintenance of intratumoral androgens in metastatic prostate cancer: a mechanism for castration-resistant tumor growth. Cancer Res 2008;68:4447-54.
31. Gribbestad IS, Sitter B, Lundgren S, et al. Metabolite composition in breast tumors examined by proton nuclear magnetic resonance spectroscopy. Anticancer Res 1999;19:1737-46.
32. Bjelakovic G, Gluud LL, Nikolova D, et al. Vitamin D supplementation for prevention of mortality in adults. Cochrane Database Syst Rev 2014;(1):CD007470.
33. Lappe JM, Travers-Gustafson D, Davies KM, et al. Vitamin D and calcium supplementation reduces cancer risk: results of a randomized trial. Am J Clin Nutr 2007;85:1586-91.
34. Bathen TF, Jensen LR, Sitter B, et al. MR-determined metabolic phenotype of breast cancer in prediction of lymphatic spread, grade, and hormone status. Breast Cancer Res Treat 2007;104:181-9.
35. Bjartell AS, Al-Ahmadie H, Serio AM, et al. Association of cysteine-rich secretory protein 3 and beta-microseminoprotein with outcome after radical prostatectomy. Clin Cancer Res 2007;13:4130-8.
36. Schubert SM, Arendt LM, Zhou W, et al. Ultra-sensitive protein detection via Single Molecule Arrays towards early stage cancer monitoring. Sci Rep 2015;5:11034.

Cite this article as: Xin H, Wang WQ, Yang ZW, Liu JX, Li S, Wang L, Jiang QL, Jia LL. Metabolomics studies of prostate cancer using gas chromatography-mass spectrometery. Transl Cancer Res 2016;5(3):302-314. doi: 10.21037/tcr.2016.06.15

